Electrical Power and Energy Systems 119 (2020) 105874

Contents lists available at ScienceDirect

Electrical Power and Energy Systems

journal homepage: www.elsevier.com/locate/ijepes

Highly reliable overcurrent protection scheme for highly meshed power systems

Ahmad Darabi[a,*], Mehdi Bagheri[a], Gevork B. Gharehpetian[b]

[a] Electrical Engineering Department of Nazarbayev University, Astana, Kazakhstan
[b] Electrical Engineering Department of Amirkabir University of Technology, Tehran, Iran

ARTICLE INFO

Keywords:
Distributed generation (DG)
Nonlinear programming (NLP)
Directional overcurrent relay (DOCR)
Objective function (OF)

ABSTRACT

To improve the transient stability of synchronous generators, overcurrent relays should react to electrical faults as fast as possible. In some cases, the backup relays cannot be coordinated properly with their primary relays using non-communication overcurrent protection schemes. In this study, a highly reliable overcurrent protection scheme is proposed to overcome this problem. Firstly, criteria are proposed to identify the pairs in which the backup relays fail to react to faults in some fault locations and communication links are used for preserving the coordination. Then, a novel optimization method is proposed, which consists of metaheuristic and deterministic parts. Although a well-known equation is used to obtain critical clearing time for overcurrent coordination in the literature, only fault at busbar is taken into account using this equation. Moreover, the postfault network topology has a significant effect on the transient stability of synchronous generators. In this research, the transient stability is analyzed for faults at different distances from overcurrent relays. Moreover, the circuit breaker operation and network reconfiguration are taken into account for finding the critical clearing time. As a result, the transient stability of the synchronous generator is improved. The proposed algorithm is applied to both the 33 kV distribution part of the 30 and 39-bus transmission IEEE standard test systems. It is shown that the relays operating and pairs discrimination times are significantly reduced. For the 30-bus power system, the obtained total relays operating time using the proposed method satisfying a highly reliable coordination is less than 1/10 of those obtained from conventional coordination methods. It is shown that, the total relays operating time obtained for the 39-bus power system considering non-zero fault impedance was dropped, and it came to the range of the obtained results for the 30-bus system using conventional methods and zero fault impedance.

1. Introduction

The increase in the number and capacity of DGs has led to several changes in the direction and magnitude of fault currents, and consequently, the priority of relay operation has changed. Thus, overcurrent relays have become directional, but changes in the magnitude of fault currents have led to destructive effects on power protection [1–4]. Generally, sensitivity, selectivity and reliability are important scopes of all overcurrent coordination schemes. That is, directional overcurrent relays (DOCRs) should be sufficiently sensitive to electrical faults to mitigate the propagation of fault damage to the other parts and to avoid transient instability of DGs [1,5–8]. In addition, all relays should operate in their corresponding zones to avoid an unnecessary outage. In fact, DOCRs should be coordinated such that the backup relay operates subsequent to its primary relay after the elapse of a specific time called the coordination time interval (CTI), which is 0.3 s in this paper. Promising research on this topic has been published, and the reported methods can be categorized into two optimization-based groups. The first proposed group includes new protection schemes (adaptive, communication based dual setting, planning, etc.) [1–3,7,9–16] or some modifications in the power system (DG and fault current limiter sizing and locating, fault ride through control of inverters, etc.) [4,13,17–29]. These methods are occasionally followed by new optimization algorithms applied to obtain relay time setting multipliers (TSMs) and plug setting multipliers (PSMs). In the second group, only new optimization algorithms are applied to the non-communication overcurrent coordination problem [14,30–51]. However, non-communication based methods cannot make DOCRs enough sensitive and fast for large power networks considering transient stability issues. Thus, new algorithms using communication infrastructure [52] without any need for optimization at the expense of higher costs have been proposed to improve relay sensitivity [7,8]. In addition, a fast relaying structure based on

* Corresponding author.
E-mail addresses: ahmad.darabi@nu.edu.kz (A. Darabi), mehdi.bagheri@nu.edu.kz (M. Bagheri), grptian@aut.ac.ir (G.B. Gharehpetian).

https://doi.org/10.1016/j.ijepes.2020.105874
Received 13 September 2019; Received in revised form 2 December 2019; Accepted 18 January 2020

fault current direction is proposed in [53]. In summary, all of these methods suffer from at least one of the following six issues.

First, the optimizer should be selected such that primary relay operating times are minimized while the discrimination times approach zero. Consequently, the global best solution should be found. This is a challenging task considering the nonconvex and nonlinear properties of the overcurrent coordination problem. Moreover, the weaknesses of nonlinear programming (NLP), linear programming (LP) and metaheuristic methods (which are discussed in more detail in Section 3.1) make the situation more complicated [14,30–38]. Second, in case of large power networks and high DG penetration, in all non-communication schemes, DGs cannot be rescued from instability after clearing the fault. Third, considering only near-end faults cannot guarantee the coordination of relay pairs for far-end faults [1,13,32–36]. Fourth, although the pickup current of DOCRs has frequently been considered lower than the minimum fault current, in some cases (especially for backup relays in the case of far-end faults), the measured fault current can be even lower than the relay load current. Thus, coordination is even impossible in this case. Fifth, overcurrent coordination based on only the fault current magnitude without any attention to the fault current direction may lead to the creation of an invisible or a blocked zone for the backup relay. Thus, the backup relay senses no fault current in this invisible zone, and consequently, no command is sent to the backup circuit breaker. Sixth, for the sake of increasing relay sensitivity, communication-based approaches have been proposed in some papers; however, utilizing communication infrastructure for all relays increase costs and lead to a variety of reliability issues [7,8].

These issues are individually focused in this paper, and notable improvements are achieved by both the proposed optimization method and the proposed coordination scheme. The first problem is eliminated by combining metaheuristic and NLP methods in a suitable manner. The gravitational search algorithm (GSA) [33], differential evolutionary algorithm (DE) [10] and conventional genetic algorithm (GA) are selected as the metaheuristic part. On the other side, Rosen's gradient projection (RGP) and Zoutendijk's method [54] are chosen for the NLP part of the optimizer engine. Although these algorithms may increase the complexity of the proposed method, they augment both exploration and exploitation of the optimizer, significantly. Thus, both primary relay operation times and the discrimination times between relay pairs are effectively minimized. The advantages of the RGP and Zoutendijk's optimization methods and their combination with metaheuristic approaches are thoroughly discussed in [38,55] and they are out of this study discussion. To overcome the second problem, a valuable nonstandard relay curve proposed by [56] is deployed in this paper. However, in the following sections, it will be discussed that utilizing the recent nonstandard relay characteristic is not sufficient to preserve desirable coordination between the relay pairs. An ancillary protection scheme is required to support the pair coordination against unpredicted changes in fault current magnitude. To satisfy the third problem, both near-end and far-end coordination constraints are considered. Thus, more reliable results can be achieved. The last three protection problems can only be removed by communication links, which are demonstrated in detail in later sections. In this study, minimum communication links are used, and excessive costs are avoided. Following, utilizing the proposed protection scheme and optimization algorithm; the synchronous generators transient stability for the emulated faults are satisfied. This occurs for distant faults from DOCRs. In the next section, coordination constraints and objective functions (OFs) are introduced. In Section 3, both the proposed optimization algorithm and proposed overcurrent protection scheme are presented. Section 4 is devoted to simulation results, and the last section is the conclusion.

2. Problem formulation

2.1. Relay curves

The general standard form of overcurrent relay curve is [57]:

$$t_{op} = \frac{A \times TSM}{\left(\frac{I_f}{I_{pickup}}\right)^B} \tag{1}$$

Given the curve proposed by [56], the utilized nonstandard form of the overcurrent relay curve is:

$$t_{op} = \left(\frac{1}{e^{1-V_f}}\right)^K \left(\frac{A \times TSM}{\left(\frac{I_f}{I_{pickup}}\right)^B}\right) \tag{2}$$

where I_f is the fault current seen by the DOCRs and I_{pickup} is the pickup load current ($PSM.I_{loadmax}$). The coefficient K is individually determined via the metaheuristic part for each DOCR. Also, the V_f is the per-unit measured voltage at DOCR location. In [56], the impacts of V_f and K on t_{op} are demonstrated. DOCRs are classified in three categories: Standard Inverse (SI), Very Inverse (VI) and Extremely Inverse (EI) relays (Table 1).

2.2. Objective functions and constraints

The proposed OFs are given by:

$$O.F_{metaheuristic} = k_1 \hat{A}\cdot MN + \sum_{i=1}^{PN} (t_{imn}{}^2 + t_{ibf}{}^2) + \sum_{i=1}^{PN} \{k_2(|\Delta t_{in} - |\Delta t_{in}||) + |\Delta t_{if} - |\Delta t_{if}||) + (\Delta t_{in} + |\Delta t_{in}|)t_{ibn}{}^2 + (\Delta t_{if} + |\Delta t_{if}|) t_{ibf}{}^2\} \tag{3}$$

$$O.F_{nonlinear} = \sum_{i=1}^{RN} (t_{imn})^2 + \sum_{i=1}^{RN} (\Delta t_{in})^2 \tag{4}$$

$$\Delta t_i = t_{ib} - t_{im} - CTI \tag{5}$$

where $k_1$and k_2 are 10^6 and 10^3, respectively. *MN*, *RN* and *PN* are the miscoordination number, total relay and pair numbers, respectively. *n* and *f* indicate the near-end and far-end faults, and *m* and *b* indicate the main and backup relays. The discrimination time is defined by (5) for both near- and far-end faults. $O.F_{metaheuristic}$ and $O.F_{nonlinear}$ were selected based on the metaheuristic and NLP features, respectively. It should be mentioned that metaheuristic algorithms are problem independent and they can be utilized for both linear and nonlinear optimization problems. In addition, these approaches are superior to find a convex vicinity of optimum points. However, convex vicinities [54] of optimum points are some solutions which satisfy the preliminary coordination constraints. Therefore, all pair miscoordinations should be eliminated using the metaheuristic part to satisfy fundamental objectives. Consequently, $O.F_{metaheuristic}$ should be compatible with this property. The presence of k_1 and k_2 supports $O.F_{metaheuristic}$ limitations for violations. In fact, $k_1(10^6)$ and $k_2(10^3)$ have made $O.F_{metaheuristic}$ highly sensitive to any miscoordination presence. Moreover, the second goal of the overcurrent coordination is to exploit the exact optimum point after finding its convex vicinity. On the other hand, it is more convenient to exploit the exact optimum solution mathematically using

Table 1
IEC 255-4 standard relays [57].

Relay Type	*A*	*B*	Standard
Normally inverse	0.14	0.02	IEC
Very inverse	13.5	1	IEC
Extremely inverse	80	2	IEC

the deterministic approaches. However, the exact optimum is a specific solution of which the relays operating times are minimum, satisfying the coordination constraints. Hence, $k_1$and k_2 can decrease the impact of$\sum_{i=1}^{PN}(t_{imn}{}^2 + t_{ibf}{}^2)$ and $\sum_{i=1}^{PN}\{(\Delta t_{in} + |\Delta t_{in}|)t_{ibn}{}^2 + (\Delta t_{if} + |\Delta t_{if}|)t_{ibf}{}^2\}$ by increasing the importance of *MN* and$\sum_{i=1}^{PN}\{(|\Delta t_{in} - |\Delta t_{in}|| + |\Delta t_{if} - |\Delta t_{if}||)\}$ in $O.F_{metaheuristic}$. Consequently, the algorithm exploration is augmented using this fitness function. Hence, $O.F_{metaheuristic}$ is appropriate for the metaheuristic part.

Minimizing relays operating and pairs discrimination times without considering miscoordinations make $O.F_{nonlinear}$ appropriate for the deterministic part. It is worth noting that although the deterministic part can only be implemented for feasible initial points without any constraint violation, all coordination constraints remain satisfied in each step of the deterministic section because of the inherent properties of the NLP methods. Hence, the term$\sum_{i=1}^{PN}\{(|\Delta t_{in} - |\Delta t_{in}|| + |\Delta t_{if} - |\Delta t_{if}||)\}$ has been eliminated from $O.F_{nonlinear}$ and consequently, prior objectives of overcurrent coordination which are reducing primary relays and pairs discrimination times are emphasized in this fitness function. It should be mentioned that in a convenient pair coordination, the backup protection should react exactly after its primary relay with a CTI time difference. For the reaction time difference exceeded from CTI; the fault damages will propagate through the network faster. Therefore, Δt should be minimized in both (3) and (4) where TSM, PSM and *K* are optimization variables. All constraints are as follows [47]:

$$\Delta t_{in} \geq 0 \quad \text{for i = 1:PN} \tag{6}$$

$$\Delta t_{if} \geq 0 \quad \text{for i = 1:PN} \tag{7}$$

$$1.2 \leq PSM \leq 1.6 \quad \text{for i = 1: RN} \tag{8}$$

$$TSM_{min} \leq TSM_i \leq TSM_{max} \quad \text{for i = 1: RN} \tag{9}$$

$$t_{min} \geq 0.05 \tag{10}$$

3. Proposed algorithm

3.1. Proposed optimization algorithm:

Overcurrent coordination is a nonlinear and nonconvex optimization problem, and an appropriate optimization method can lead to accurate DOCR coordination. However, each method has some deficiencies. For instance, ensuring a balance among all terms in (3) in order to eliminate miscoordination, to minimize the primary operating time and to make all discrimination times approach to zero simultaneously is a difficult task for metaheuristic algorithms. Moreover, in comparison to deterministic (i.e., LP and NLP) approaches, these algorithms have a weak exploitation capacity. On the other hand, deterministic methods also provide acceptable exploitation, and there is no need to ensure a balance between the constraints and objectives in their OFs. Since the constraints are considered in the main structure of these methods. However, the exploration property of deterministic methods is weak, and these methods are suitable for only convex problems. Clearly, only a nonlinear fitness function can minimize the primary operating times and obtain discrimination times approaching zero simultaneously. Therefore, the combination of metaheuristic and deterministic (NLP) methods can compensate for their weaknesses. In this case, optimized values for TSMs can be achieved by the NLP part and the other design variables can be achieved by the metaheuristic part.

It should be mentioned that implementing different population-based and NLP approaches to optimize design variables improves the exploration and exploitation of the optimizer. However, the selection of these optimization approaches should be fulfilled based on the requirements and features of the overcurrent coordination problem. Optimal solution for TSMs can be achieved using the NLP part, however, PSMs should be constant in each loop in the NLP algorithm. On the other hand, if TSMs are considered as the only design variables, overcurrent coordination becomes an optimization problem with nonlinear fitness function and linear constraints based on Eqs. (4), (6), (7), (9) and (10). Hence, an NLP method applicable for optimization problems with nonlinear fitness function and linear constraints (i.e., RGP) suits overcurrent coordination to optimize TSMs [54].

More complementary explanation is given in our recent study [38]. Based on the aforementioned concept, the proposed combinatorial optimization method in [38] obtains a desirable coordination. The obtained relays operating times are in the range of dual setting communication assisted methods using only SI relays, without any requirement to communication infrastructure. RGP and Zoutendijk's method are two of the best NLP methods that have the required properties for the overcurrent coordination problem. In the proposed algorithm, GSA [33], DE [10], and conventional GA are executed in a parallel manner with (3) as the OF. That is, each of these algorithms is implemented separately, and then the n population with the lowest OF is selected from the total generated population by GSA, DE and GA for the next iteration. Hence, each population is exposed to all these metaheuristic methods and all chances for finding the global optimum are considered. After removing all violations by the metaheuristic part, the RGP is implemented with the OF_1 given by (4) after each iteration of the metaheuristic part. This loop is iterated until no change is observed, and then Zoutendijk's method is implemented. Similar to RGP, Zoutendijk's method is used to obtain only TSMs because implementing Zoutendijk's method to obtain both TSMs and PSMs consumes an excessive amount of time. The proposed algorithm is depicted as Fig. 1.

3.2. Proposed coordination scheme

Based on the fault distance from the primary relay, the backup relay experiences four different protection zones: desirable, undesirable, invisible and blocked protection zones, which are indicated by DPZ, UPZ, IPZ and BPZ, respectively, in this paper. Based on these protection zones, relay pairs can be categorized into different cases as following.

- Case A: This case is the most common case among relay pairs. In this case, the minimum fault current seen by the backup relay is more than 1.6 times larger than the relay load current. Therefore, all faults with different distances from the primary relay are in the DPZ. Non-communication overcurrent scheme can coordinate pairs in this case such that the relay pickup current can be chosen from [$1.2I_{load}$ $1.6I_{load}$].
- Case B: This case is very common among relay pairs. In this case, the $I_{faultmin}$ seen by the backup relay is between $1.2I_{load}$ and $1.6I_{load}$, and the backup relay pickup current can be chosen from [$1.2I_{load}$ $I_{faultmin}$]. Traditional overcurrent coordination roles can coordinate pairs in this situation.
- Case C: This case is similar to case B; that is, the $I_{faultmin}$ seen by the backup relay is between $1.2I_{load}$ and $1.6I_{load}$ and very close to $1.2I_{load}$. In this case, based on the fault distance from the primary relay, the backup relay experiences fault in DPZ or UPZ. For instance, pair R_{57}-R_{52} is chosen from the 39-bus standard transmission test system (provided in Section 4). The fault current measured by R_{52} based on fault distance from R_{57} is depicted in Fig. 2. As shown in Fig. 2, in the case of a far-end fault, R_{52} measures 991 (A), while the R_{52} load current is 762 (A).

That is, if the minimum load current (i.e., 1.2 I_{load}) is selected as the pickup current and if the minimum TSM (i.e., 0.05) is selected, based on SI (Table 1), R52 clears the far-end fault after 4.3237 (s). Moreover, because of coordination constraints, selecting the minimum values of

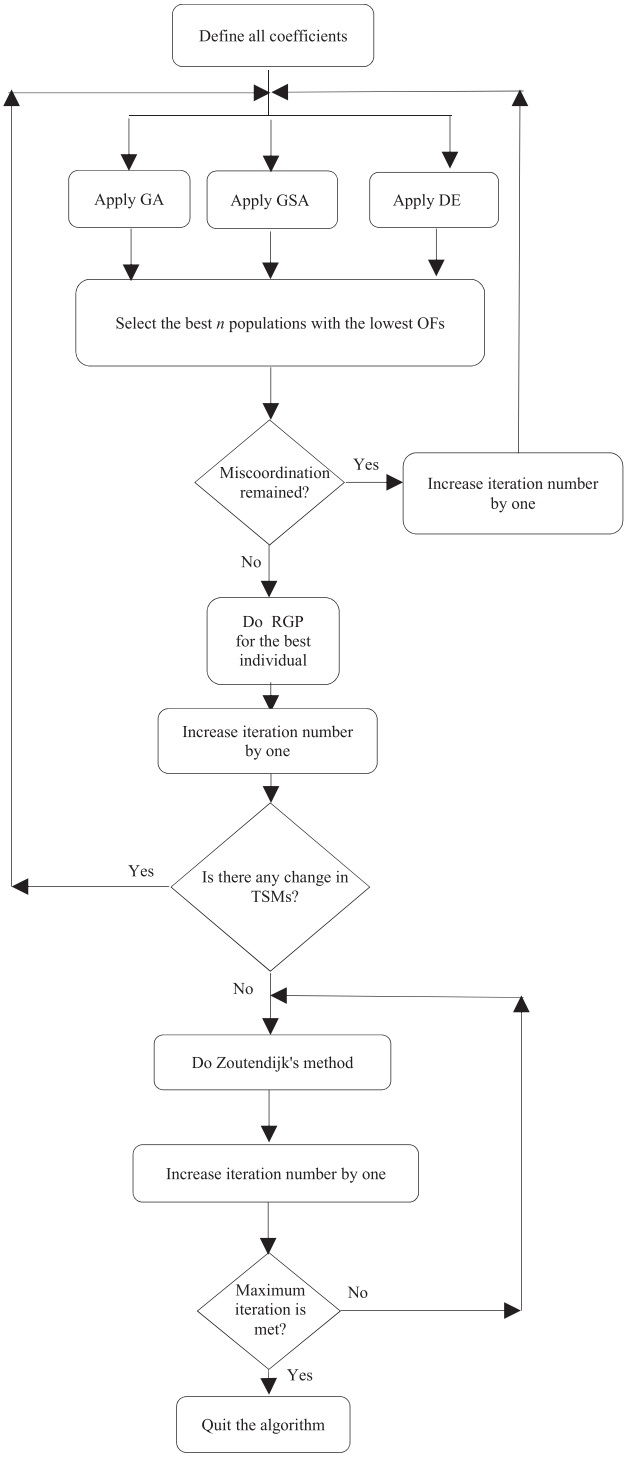

Fig. 1. The proposed optimizer.

both TSM and PSM for R52 is impossible. Thus, the far-end fault is in an undesirable zone for R52. Although R52 is an obvious example for case C, in general, pairs in this case are identified by simulation, as discussed in Section 4. This case is one for which non-communication coordination scheme fails to provide reliable coordination. A communication link is proposed to guarantee pairs coordination in this case. In summary, obvious cases are removed from the optimization problem, and other pairs can be identified by simulation.

- Case D: In this case, $I_{faultmin}$ is even lower than $1.2I_{loadmax}$. Obviously, when the fault current magnitude is lower than the minimum pickup current, the relay senses no extra current and fails to protect the power system. This case is more likely for the backup relay in the case of far-end faults. This problem appears when faults with different locations are considered instead of only near-end faults. Only near-end faults have been frequently considered in the literature; however, this consideration leads to the creation of a UPZ or BPZ for the backup relay in case of different fault distance from the primary relay, see Fig. 3. Thus, a communication link is proposed to preserve the coordination. These pairs can be identified by comparing the fault current magnitude with $1.2I_{load}$. R53-R51 in the 39-bus standard transmission test system is an illustrative example for case D (Fig. 3).
- Case E: In comparison to the previous cases, this case is very critical but has attracted less attention in the literature. In this case, the measured far-bus current by the backup relay can be greater than $1.2I_{load}$ or even $1.6I_{load}$ (e.g., R1-R3 for 39-bus system). The far-bus current magnitude measured by the backup relay can be even greater than the near-bus current magnitude measured by the backup relay (e.g., R6-R4 for 39-bus system). For an occurred far-end fault, we would have similar optimization cases as A and B, if the only sensed fault current magnitude by the backup relay without regarding fault current direction is considered. However, this case fundamentally differs from cases A and B. Specifically, the direction of the fault current seen by the backup relay changes as the fault distance from the primary relay becomes greater than a specific value. Thus, after this specific distance, the backup DOCR is blocked for faults in the reverse direction. Fig. 4 is a small part of the 39-bus system and indicates the case in which the far-bus current measured by the backup relay is greater than the near-bus current measured by the backup relay. Pairs R_5-R_1 and R_6-R_4 are appropriate examples for this case. For instance, the fault current measured by R_4 for faults with different distances from R_4 is plotted in Fig. 5.

In case E, all protection zones are possible. For instance, the fault current magnitudes seen by R_4 and R_1 based on the fault distance from R_6 and R_5 are plotted in Fig. 5 and Fig. 6, respectively. As shown in Figs. 5 and 6, the fault current direction observed by R_4 and R_1 changes when the fault distances exceed 28 and 35 percent of the corresponding line p.u. from R_6 and R_5, respectively. Thus, after this point, R_4 and R_1 are not allowed to react. In pairs R_5-R_1 and R_6-R_4, the fault current magnitudes seen by the backup relay for far-end faults are greater than those for near-end faults. Hence, these pairs can be identified easily; however, this is not always the case for the pairs in case E. For instance, R_1-R_3 can be selected, and Fig. 7 is obtained after plotting the fault magnitudes seen by R_3 for different fault distances from R_1. As shown in Fig. 7, after 73 percent of the line distance, the fault current direction changes, and the far-end fault current magnitude is slightly more than $1.6I_{loadmax}$. Thus, another criterion is needed. The second criterion is that the fault current measured by the backup relay should be a decremental function of fault distance from the primary relay. However, plotting the faults measured by all backup relays for all possible locations takes a long time. It is proposed that the current magnitude seen by the backup relay for both 100 percent of the line length (far-end) and (100-ε) percent of the line length can be calculated without considering the current phase passing from the backup relay. If the measured current is increasing in this space, the redundant coordination constraint is proposed to be equipped with a communication link since the non-communication coordination scheme fails to coordinate pairs in this case.

- Case F: This case is critical only when DOCRs are coordinated by the proposed nonstandard curve by [37]. In other words, this case has no impact on coordination by relays with standard characteristics. Bus voltages can impact pair coordination in the case of non-standard curves. In typical relay pairs, the voltage of the primary relay busbar is lower than the voltage of the backup relay busbar in

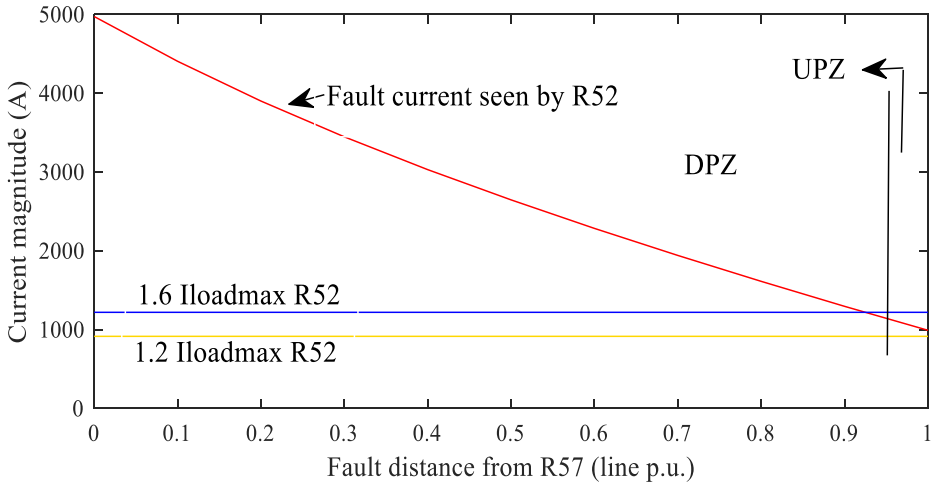

Fig. 2. Case C: $I_{faultmin} < 1.6I_{load}$, and $I_{faultmin}$ is close to $1.2I_{load}$.

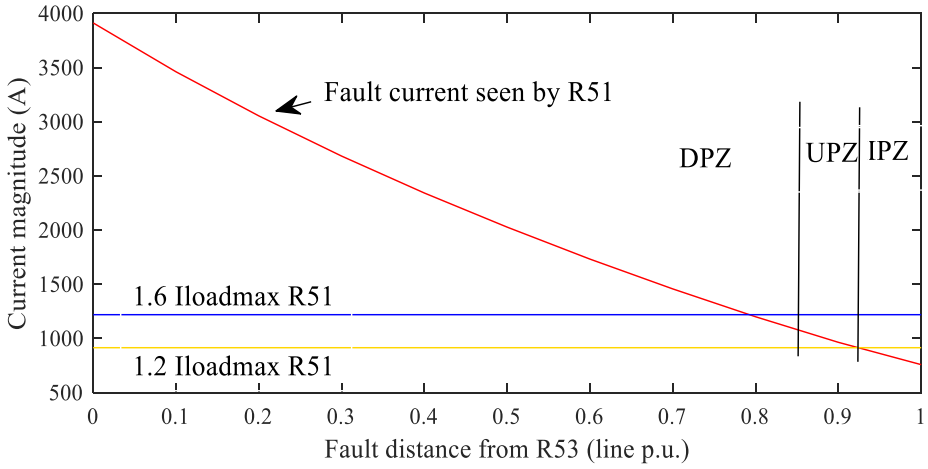

Fig. 3. Case D: $I_{faultmin} < 1.2I_{load}$.

the case of a far-end fault. If this is not the case for a specific pair, then that pair is removed from the coordination optimization problem, and a communication link is proposed to preserve the coordination. The primary and backup busbar voltages for a typical case (R_7-R_1) and a pair in case F (R_6-R_4) for the 39-bus system are plotted in Figs. 8 and 9, respectively.

4. Simulation and results

The proposed algorithm is applied to the 33 kV distribution part of the 30-bus (Fig. 10) and to the 39-bus transmission (Fig. 11) standard test systems. Simulations show that the best alternative for relay curves is (2) while only SI characteristics are selected for coefficients A and B (Table 1).

The fault current contribution of inverter-based DGs can significantly be controlled [4,23–25]. Hence, only synchronous generators (SGs) are considered for DOCR coordination. To obtain the critical clearing time (CCT) of a specific SG for a fault occurring at a specific line, first, the fault with a desirable distance from the SG is located at the line. Then, after an elapsed period of time, the line circuit breaker is opened. If after de-energizing the line, the corresponding SG can become stable, then the time difference between the fault initiation and circuit breaker reaction is increased. This process is continued until the time difference between fault initiation and circuit breaker reaction becomes high enough that the SG can never be stable after de-energizing the line. This time difference is known as the CCT of the corresponding SG.

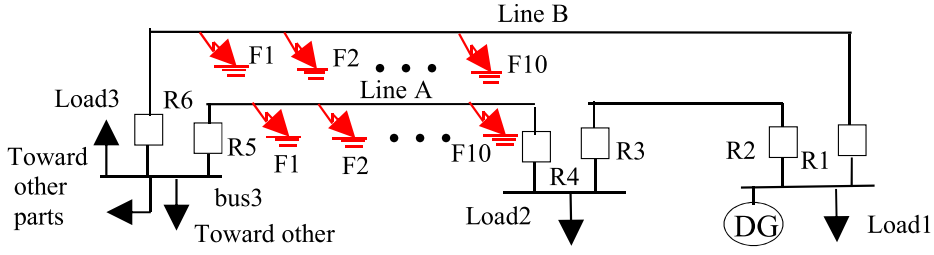

Fig. 4. Case E: A small part of the 39-bus transmission system.

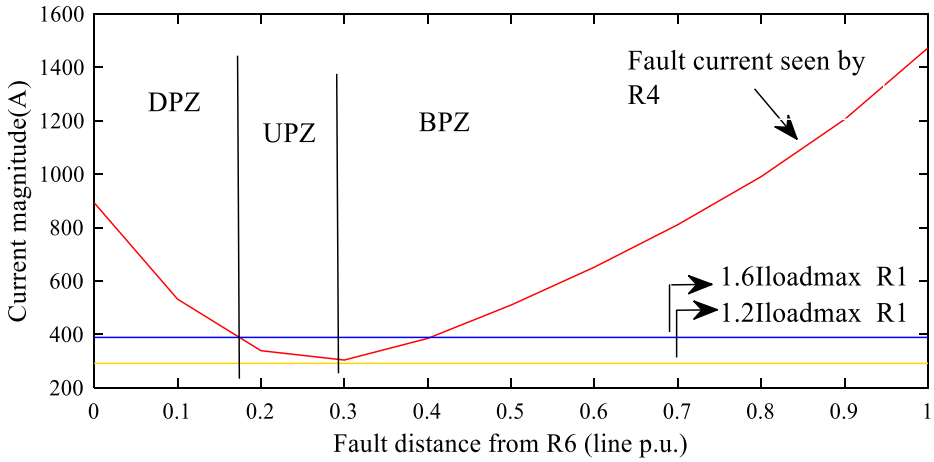

Fig. 5. Protection zones of R_4 based on fault distance from R_6.

4.1. The 33 kV distribution part of 30-bus power system

This network has 38 DOCRs and 58 relay pairs [5]. The network data can be found in [58]. Three SGs are connected to buses 7, 15 and 10 with nominal apparent powers of 8, 9 and 6 MVAs and inertia constants of 0.9, 1 and 0.5 s, respectively. Based on Section 3.2, non-communication coordination schemes can coordinate pairs in cases A, B and C. However, in case C, high values of the discrimination time cannot be obtained, and coordination is not reliable. Cases D, E and F, which cannot be coordinated with non-communication scheme, are gathered in Table 2. Based on this table and the proposed coordination scheme, 7 pairs are coordinated by communication links, and the other 51 pairs are coordinated by the proposed optimization method, as shown in Table 3. Table 3 shows that the obtained total relays operating time (i.e., 5.38 s) using a highly reliable coordination scheme is significantly reduced. It became to less than 1/10 of the obtained total relays operating time using the conventional coordination scheme (64.172 s in [5], 64.710 s in [59]) for the same power system. Moreover, the new result is in the range of 1/6 of those provided by dual setting coordination schemes (34.172 s in [5], 30.94 s in [7]). The obtained result using the proposed method is compared with the results achieved implementing the other approaches reported in the literature in Table 4. It is worth mentioning that the obtained results satisfy overcurrent coordination for both near- and far- end faults.

In Table 3, the last column indicates the length of feeders in which the installed overcurrent relays can rescue the corresponding DGs from instability. For a specific fault on L_{11}, R_{30} should react fast enough such that SG_3 can recover its stability after de-energizing L_{11}. To determine this specific distance, the following process should be implemented for L_{11} which is the same for other feeders and SGs:

First, 11 faults should be emulated with the same distances on L_{11} such that the first fault is emulated very close to bus 10 (in front of R_{30}) and the eleventh fault is simulated very close to bus 11 (in front to R_{11}). Then, all fault currents and busbar voltages for all the simulated faults are collected.

Subsequently, relays operating times for all the emulated 11 faults (0% of L_{11}, 10% of L_{11}, …, 100% of L_{11}) should be calculated as t_0, t_{10}, …, t_{100} using the collected currents and voltages and the provided values of TSM, PSM and K in Table 3. In the next step, a fault is simulated in front of R_{30} (0% of L_{11}) and R_{30} circuit breaker is manually tuned (in the simulation process) to de-energize L_{11} after the fault initiation time with a time duration equal to t_0. In the next step, stability condition of SG_3 is checked after disconnection of L_{11}. If SG_3 cannot be stabilized after circuit breaker operation, R_{30} cannot rescue SG_3 even for occurred faults in front of R_{30}. Otherwise, the stability condition should be checked for another fault occurred in 10% of L_{11}. This process continues up to the point that SG_3 cannot recover its stability after removing the fault by R_{30} beyond this point. In particular, Table 3 shows that DOCRs could satisfy the stability of the all connected SGs in the 30-bus IEEE standard power system. However, the following section shows that in several cases, DOCRs cannot satisfy the transient stability of the corresponding SGs after fault elimination for the 39-bus standard power transmission network.

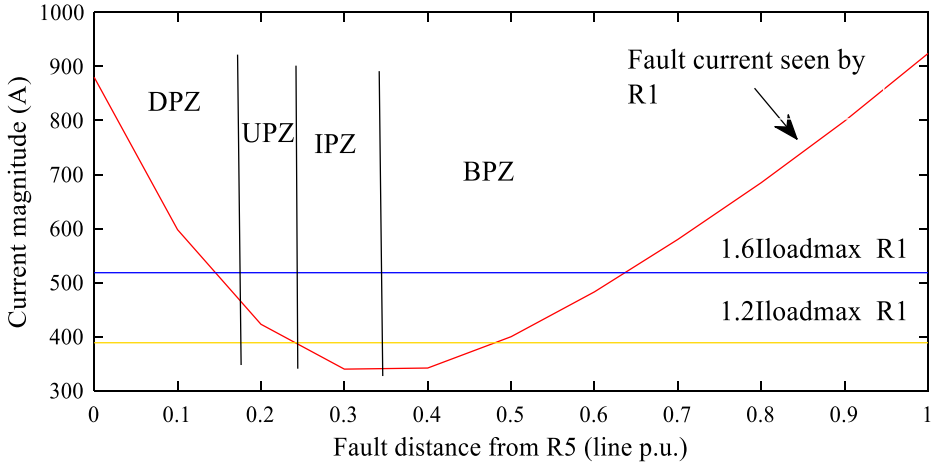

Fig. 6. Protection zones of R_1 based on fault distance from R_5.

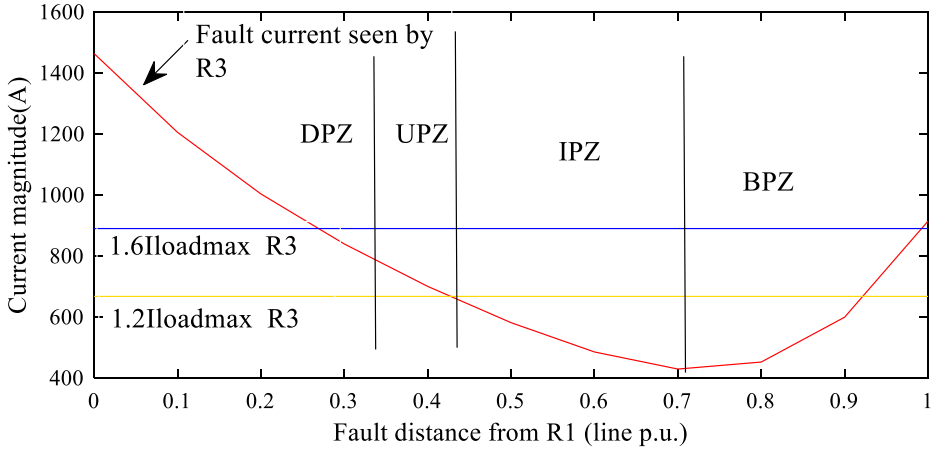

Fig. 7. Protection zones of R_3 based on fault distance from R_1.

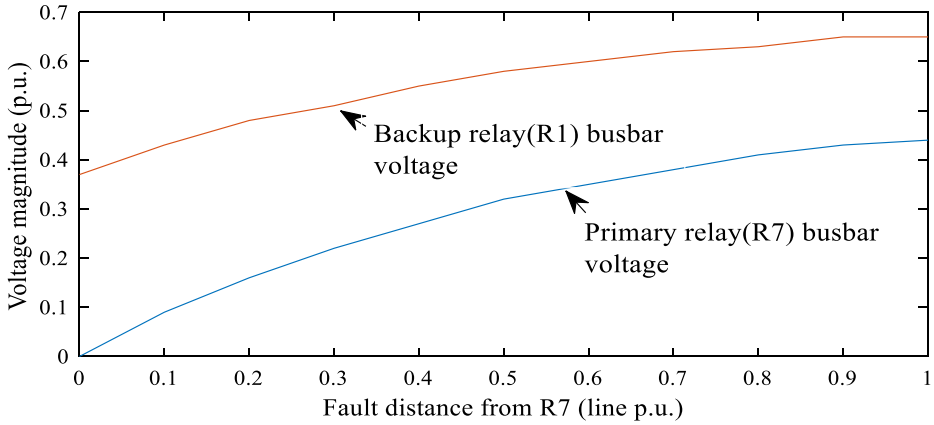

Fig. 8. Primary and backup relays busbar voltages for a typical case.

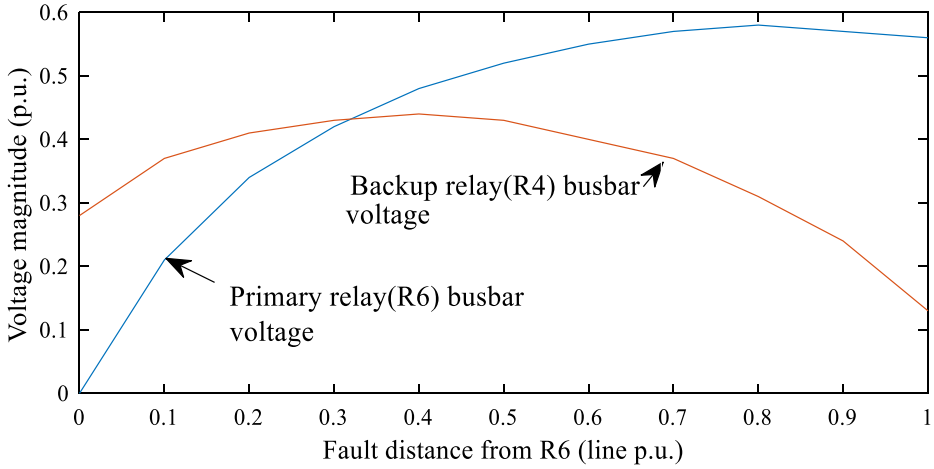

Fig. 9. Primary and backup relay busbar voltages for case F.

4.2. The 39-bus standard system

This network has 66 relays and 106 relay pairs (Fig. 11). Based on the proposed method, 9 relay pairs are dropped from the coordination (Table 5 plus R_{57}-R_{52} as case C). The obtained results for this network are gathered in Table 6.

For a paired validation, mid-way faults with 10 Ω impedance were located at all the lines and the proposed method was examined. Table 7 shows the results of this new evaluation. As demonstrated in Table 7, the total relays operating time for the standard 39-bus power system (i.e., 62.2919 s) is in the range of the obtained result for the 30-bus system using conventional methods and zero fault impedance (64.172 s in [5], 64.710 s in [59]).

4.3. Results and discussion

The following section contains some important notes. First, although the nonstandard equation [56] used for relay characteristics reduces relay operating times, without an appropriate optimization algorithm, achieving acceptable results is impossible. The proposed

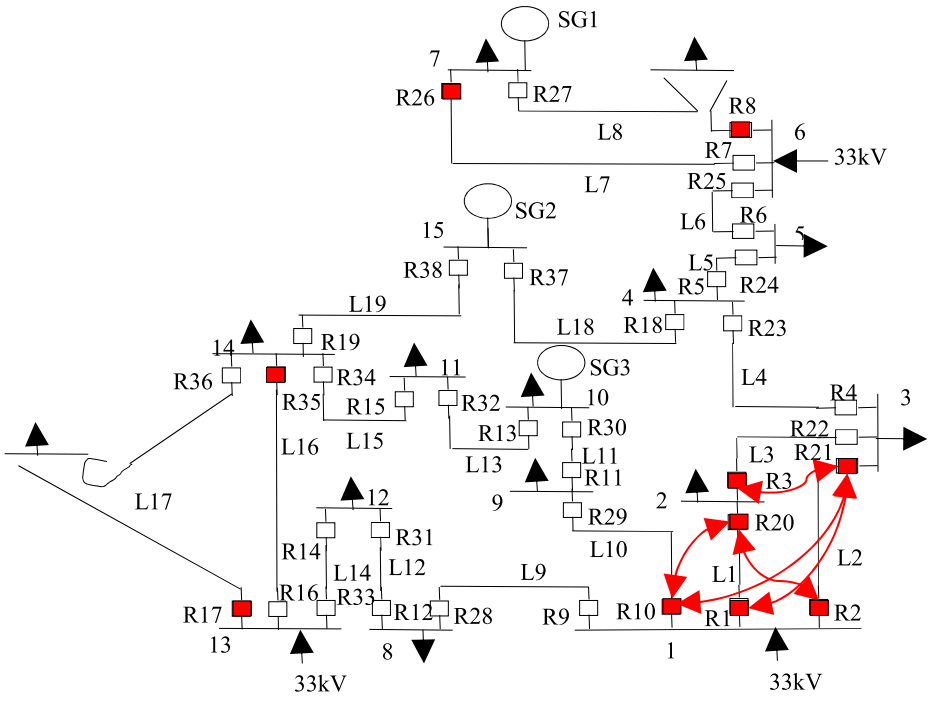

Fig. 10. 33 kV distribution part of the 30-bus power network.

optimizer engine consists of both metaheuristic (for optimizing K and PSM values) and deterministic components (for optimizing TSM values). Consequently, both the exploration and exploitation of the optimizer engine are augmented such that the relay operating times considering their corresponding constraints are gathered in a narrow band (Tables 3 and 6). Second, although different optimization methods have been embedded in the proposed optimizer, they all led to find the global optimum with less iterative loops. The proposed optimizer engine was converged within 70 iterations, hence, it is applicable for large power networks. Third, although increasing the maximum value of K in (2)

Table 2
Pairs proposed to be coordinated by communication links (30-bus standard system).

	Pairs
Case D	R_{10}-R_{20}, R_{10}-R_{21}
Case E	R_{21}-R_3, R_2-R_{20}, R_1-R_{21}, R_8-R_{26}, R_{17}-R_{35}
Case F	R_{21}-R_3, R_2-R_{20}, R_1-R_{21}, R_8-R_{26}, R_{17}-R_{35}, R_{10}-R_{20}

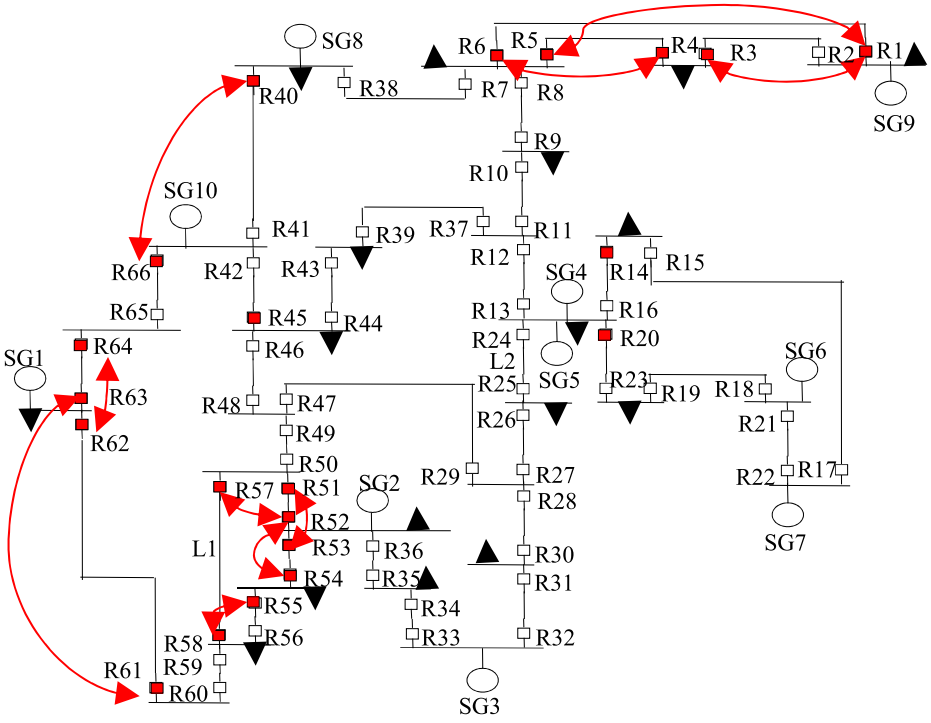

Fig. 11. The 39-bus transmission power network.

Table 3
Results obtained for the 33 kV part of the 30-bus network.

RN	TSM	PSM	*K*	$t_{near-end}$	$t_{far-end}$	transient stability
1	3.3130	1.3729	3.6815	0.1805	0.5765	
2	2.4400	1.3167	3.0683	0.1921	0.6674	
3	3.2714	1.3395	2.9814	0.2765	0.3500	
4	2.9916	1.4525	4.5859	0.0500	0.4337	
5	2.6434	1.3639	4.4144	0.0500	0.6441	
6	3.0349	1.3647	4.1356	0.1184	0.3500	
7	2.8726	1.4159	4.5990	0.0500	0.9070	SG1 100% of line
8	1.5665	1.3848	3.9784	0.0500	0.5329	
9	3.6093	1.3603	4.4550	0.0778	0.3831	
10	2.9658	1.4305	4.6362	0.0500	0.7907	
11	3.0488	1.4131	3.0261	0.2949	0.4931	SG3 100% of line
12	3.1715	1.3815	4.0837	0.0831	0.4608	
13	3.3122	1.3582	3.2814	0.1931	0.4465	SG3 100% of line
14	2.4526	1.3940	3.8059	0.1224	0.3651	
15	3.3615	1.3615	3.8932	0.1465	0.4254	
16	2.7373	1.4001	4.4908	0.0651	0.3918	
17	2.6356	1.3372	4.4592	0.0500	0.6993	
18	2.6053	1.2895	3.9833	0.0792	0.4975	SG2 100% of line
19	3.8150	1.3907	4.4950	0.0519	0.4118	SG2 100% of line
20	1.1737	1.2115	3.4020	0.1176	0.3778	
21	3.2566	1.4431	4.3579	0.0840	0.3778	
22	2.2101	1.4204	2.4282	0.3392	0.4176	
23	3.0734	1.3721	3.1977	0.2444	0.6392	
24	3.6572	1.3749	4.0239	0.1261	0.5444	
25	4.3147	1.4510	4.8770	0.0702	0.4261	
26	1.7778	1.3782	4.0721	0.0764	0.3702	SG1 100% of line
27	1.7799	1.3846	4.1769	0.0500	0.2254	SG1 100% of line
28	1.3557	1.2005	2.4682	0.3388	0.4921	
29	2.0661	1.4218	3.3606	0.1994	0.4921	
30	2.2297	1.3071	2.6379	0.3522	0.4994	SG3 100% of line
31	3.8509	1.3910	3.3283	0.2437	0.6795	
32	3.7802	1.4387	2.9177	0.3345	0.6522	SG3 100% of line
33	3.3186	1.4259	4.7361	0.0500	0.6413	
34	2.5700	1.4008	3.8411	0.0918	0.6345	
35	2.4047	1.2008	3.8788	0.1254	0.3500	
36	2.4826	1.3845	3.9270	0.0500	0.3645	
37	2.9060	1.5452	3.8583	0.1118	0.5502	SG2 100% of line
38	2.8425	1.4021	3.0627	0.1906	0.4503	SG2 100% of line
		Sum:		5.3775	19.0110	100% of SGs

leads to a decrease in the relay operating times, eliminating miscoordinations by the metaheuristic part becomes more difficult. Thus, *K* cannot be increased unboundedly. Consequently, the role of the optimizer engine in the removal violations and finding prominent optimized results becomes more vital.

Fourth, the utilized fitness functions for the metaheuristic and deterministic parts have been proposed based on discussed properties and capabilities of these optimization methods in Section 3.1. It should be mentioned that coefficients k_1 and k_2 make $O.F_{metaheuristic}$ highly sensitive to miscoordinations. Hence, optimizing relays operating and pairs discrimination times are secondary functions of $O.F_{metaheuristic}$ and consequently, exploration is more augmented than exploitation via this fitness function formulation. These properties made the proposed OF in Eq. (2) appropriate to be utilized via the metaheuristic part. On the other hand, only relays operating and pairs discrimination times have been taken into account in the structure of $O.F_{nonlinear}$ and coordination constraints have been removed from this fitness function. Based on Section 3.1, these properties make the $O.F_{nonlinear}$ appropriate for the deterministic part.

Table 5
Pairs proposed to be coordinated by communication links (39-bus standard system).

	Pairs
Case D	R_{20}-R_{14}, R_{52}-R_{54}, R_{63}-R_{61}, R_{53}-R_{51}
Case E	R_5-R_1, R_1-R_3, R_6-R_4, R_{58}-R_{55}
Case F	R_5-R_1, R_1-R_3, R_6-R_4, R_{58}-R_{55}

Fifth, to achieve better results, in comparison to the chosen boundaries for the pickup currents, the chosen boundaries for the TSM and *K* variables can be more flexible. To be exact, although the relay operating times can be reduced by considering a vast boundary for pickup currents, it is not recommended because the pickup currents determine the sensitivity of the relays to faults. Thus, the standard boundary of $[1.2I_{loadmax}\ 1.6I_{loadmax}]$ is used for pickup currents. If the pickup current is lower than $1.2I_{loadmax}$, sympathetic tripping is expected, and if the pickup current is greater than $1.6I_{loadmax}$, faults with

Table 4
Obtained total relays operating time for the 30-bus power system using different coordination methods.

Method	$\Sigma t_{op\text{-}primary}$	Method	$\Sigma t_{op\text{-}primary}$
Proposed Method in [5] (Dual Setting)	33.7388 s	Proposed method in [47] (NI Relays)	64.17 s
Proposed Method in [7] Dual Setting	30.94 s	Proposed method in [47] (User-Defined)	35.06 s
Proposed Optimizer in [38] (NI Relays)	34.5636 s	Proposed method in [55] (NI Relays)	29.93 s
Proposed Optimizer in [38] (NI, VI, EI Relays)	17.1854 s	Proposed Method	5.3775 s

Table 6
Results obtained for the 39-bus network.

RN	TSM	PSM	*K*	$t_{near-end}$	$t_{far-end}$	transient stability
1	1.4162	1.3234	4.4813	0.0500	0.8133	SG9 3% of line
2	1.1461	1.3421	3.9216	0.0955	0.3518	SG9 CCT= 44 ms
3	2.1243	1.3922	5.7484	0.0500	0.1562	SG9 8% of line
4	1.5010	1.3605	4.5454	0.0518	0.3968	
5	0.2371	1.3497	1.9194	0.0756	0.3937	
6	0.4148	1.3393	2.9914	0.0500	0.6182	SG9 7% of line
7	2.5791	1.4262	4.6735	0.0500	0.5213	SG8 57% of line
8	2.4186	1.3810	4.4109	0.0968	0.4639	
9	1.9463	1.3479	4.2761	0.0911	0.3756	
10	4.2652	1.4078	3.7187	0.1639	0.4452	
11	3.4320	1.3513	4.6283	0.0500	0.5769	
12	2.5105	1.4804	3.9498	0.1452	0.4056	SG4 3% of line SG5 3% of line
13	4.3036	1.4910	5.1883	0.0586	0.4055	SG4 32% of line SG5 33% of line
14	2.5869	1.3779	3.4571	0.2497	0.3586	SG4 CCT=210 ms SG5 CCT=210 ms
15	1.5663	1.3399	4.5126	0.0500	1.0314	SG7 24% of line
16	2.5755	1.4645	3.7623	0.1056	0.3500	SG4 41% of line SG5 40% of line
17	1.4354	1.4288	4.5355	0.0500	0.9089	SG7 24% of line
18	0.7217	1.3991	3.6319	0.0862	0.4465	SG6 CCT=78 ms
19	1.7117	1.4023	4.8762	0.0668	0.4106	SG6 13% of line
20	3.1866	1.4200	5.0935	0.0500	0.6804	SG4 23% of line SG5 23% of line
21	3.5023	1.4104	4.0269	0.1106	0.3500	SG6 38% of line SG7 37% of line
22	4.8934	1.4335	4.2104	0.1486	0.3862	SG6 23% of line SG7 12% of line
23	0.9426	1.3157	3.2683	0.1465	0.4056	SG4 2% of line SG5 3% of line
24	2.4073	1.3697	4.8250	0.0500	0.4036	SG4 57% of line SG5 58% of line
25	2.3908	1.3363	4.1754	0.1766	0.4056	SG4 28% of line SG5 27% of line
26	3.3397	1.5036	4.7483	0.0500	0.4989	
27	2.4270	1.4690	3.6861	0.0941	0.5779	
28	3.4437	1.4310	3.9836	0.1875	0.6753	
29	1.8987	1.4463	3.8268	0.1237	0.4821	
30	3.1688	1.3908	4.3812	0.1302	0.4237	
31	2.5761	1.3882	3.2035	0.3753	0.5859	SG3 CCT=210 ms
32	2.6760	1.4124	3.5384	0.2397	0.4302	SG3 CCT=188 ms
33	3.3143	1.4055	3.7332	0.2859	0.5182	SG3 CCT=188 ms
34	3.0625	1.3208	3.5915	0.3194	0.5397	SG3 CCT=215 ms
35	2.2709	1.5022	3.7626	0.2182	0.5432	SG2 2% of line
36	2.9111	1.5022	3.9323	0.1899	0.6194	SG2 8% of line
37	2.6350	1.3607	4.0795	0.1055	0.3986	
38	3.6557	1.3589	4.8235	0.0500	1.2843	SG8 28% of line
39	2.7866	1.3966	3.7476	0.2019	0.4452	
40	2.4044	1.4525	4.3291	0.1102	0.3500	SG8 CCT=188 ms SG10 CCT=99ms
41	2.1529	1.3679	4.6273	0.0500	0.4201	SG8 34% of line SG10 33% of line
42	2.3362	1.3436	4.8829	0.0500	0.6454	SG10 58% of line
43	3.2884	1.4392	4.0758	0.0986	0.3574	
44	2.6675	1.4204	3.5769	0.1203	0.5284	
45	1.2912	1.2469	4.2734	0.0574	0.3500	SG10 77% of line
46	3.1143	1.3537	4.8666	0.0500	0.7230	
47	2.7751	1.4053	4.3582	0.1006	0.4875	
48	2.5265	1.4111	4.7777	0.0500	0.5091	
49	3.3816	1.4203	3.7167	0.1821	0.6624	
50	3.0444	1.3967	4.2784	0.0943	0.4006	
51	1.4073	1.3750	2.8855	0.3332	0.4899	SG2 CCT=216 ms
52	3.4766	1.3985	3.9939	0.2432	0.3943	SG2 CCT=204 ms

(*continued on next page*)

Table 6 (*continued*)

53	2.8230	1.4021	4.3776	0.1105	0.5119	SG2 37% of line
54	1.0115	1.2387	3.7625	0.1038	0.4899	SG2 67% of line
55	2.3190	1.4026	3.4738	0.2119	0.3500	
56	3.1357	1.4923	3.6151	0.2247	0.4038	
57	2.7251	1.3419	4.1574	0.1178	0.5247	
58	1.5535	1.2079	3.2548	0.1925	0.6332	
59	2.2150	1.3914	4.5243	0.0500	1.0100	
60	0.7117	1.4523	1.9004	0.2062	0.8082	
61	0.8624	1.3734	3.7383	0.0500	0.1611	SG1 100% of line
62	0.5199	1.4135	2.5452	0.0500	0.7193	SG1 100% of line
63	1.3707	1.3694	3.7212	0.0500	2.2739	SG1 100% of line
64	0.8791	1.3995	3.1613	0.1082	0.3500	SG1 100% of line
65	0.6577	1.3589	3.3934	0.0500	0.5448	SG10 73% of line
66	0.2937	1.3730	2.4026	0.0500	0.4845	SG10 100% of line
Sum				8.0056	35.667	

higher impedance are ignored. If in a specific case (especially for backup relays and considering far-end faults), $I_{faultmin}$ is lower than $1.6I_{loadmax}$, then the denominator of (2) becomes negative. Consequently, in this case, the discrimination time is negative, and this case is considered a constraint violation. Hence, this case is removed after selecting a new pickup current in the range of $[1.2I_{loadmax}\ I_{faultmin}]$ by the metaheuristic part.

Sixth, Tables 2 and 5 reveal another notable fact: all pairs in case F can be found in other cases (especially case E). Thus, no extra communication link is needed. This outcome can be justified by the fact that when the voltage of the backup relay busbar becomes lower than that of the primary relay busbar, the current direction seen by the backup relay changes. Consequently, the fault current flows from the primary relay busbar to the backup relay busbar (case E).

Seventh, in the case of far-end faults and the 39-bus network, pairs R_{66}-R_{40}, R_{66}-R_{45} and R_{62}-R_{64} have discrimination times of 15.2 s, 16.8 s and 19.54 s, respectively. Thus, these pairs can be categorized as case C, which can be coordinated with communication links. Based on the aforementioned points, pairs that are proposed to be coordinated with communication links are shown in red in Figs. 10 and 11.

Eighth, although a well-known equation has been developed for calculating the CCT of SGs [60] and is frequently used for DOCR coordination in the literature, it is obtained based on three important considerations. First, faults should occur at the bus, and faults on lines are not considered; however, in DOCRs coordination, CCTs of SGs for faults in different locations are needed. Second, the network configuration is the same prefault and postfault; however, faults should be cleared by circuit breakers. Thus, the network topology changes after de-energizing the line. Because of this condition (in the 39-bus network), the CCT of SG6 for a fault in front of R_{18} is 78 ms, while this value for a fault in front of R_{21} is 189 ms. Third, line resistances are ignored; however, this is not the case for a real network. Moreover, satisfying transient stability of synchronous generators is more complex in case of meshed networks than radial networks.

In Tables 3 and 6, the blue boxes show that the transient stability for the corresponding fault distance from the corresponding relay is satisfied. For instance, R_7 guarantees the stability of SG_8 for faults between R_7 and 57% of the line length from R_7. These results show that the transient stability of all SGs for the 30-bus network is guaranteed. The yellow boxes indicate cases in which the SGs become instable before tripping the corresponding relays (violet boxes). For some cases (SG_9 for a fault in front of R_2) where the CCT of SG (44 ms) is lower than the minimum required time (50 ms), even for an intentional fault, the SGs can never be rescued. In other words, due to the mechanical restriction of circuit breakers, it is impossible to satisfy the transient stability of SGs, no matter which coordination scheme (e.g., conventional, adaptive, dual setting, etc.) is utilized. Moreover, all faults are not permanent, and the potential to utilize recloser for meshed networks is low [61–63]. The objective of this study is focused to make the coordination highly reliable and fast enough to satisfy the transient stability of SGs. Hence, the simulated CCTs of SGs are utilized to evaluate the performance of DOCRs.

It is worth mentioning that the performance of installed relays on both sides of feeders should be taken into account to determine the transient stability of the relevant SGs. For instance, considering the 39-bus transmission power network relays R_{24} and R_{25} which have been located on both sides of L_2 typify the situation. Table 6 indicates that R_{24} can satisfy transient stability of SG_5 for the occurred faults between R_{24} and 58% of L_2 from the R_{24} side. On the other hand, R_{25} can satisfy the transient stability of SG_5 for the occurred faults between R_{25} and 27% of L_2 from the R_{25} side. Consequently, SG_5 can be rescued from transient instability for the faults emulated in 85% of L_2.

Network reconfiguration: Network reconfiguration during faulty condition is another issue which in turn potentially creates challenges for entire coordination schemes. For instance, we assume a small portion of the 39-bus standard power test system where R_{57} and R_{58} are

Table 7
Primary Operating for 10 Ω Resistance Mid-way Fault in the 39-Bus Network.

RN	$T_{mid\text{-}way}$	*RN*	$T_{mid\text{-}way}$	*RN*	$T_{mid\text{-}way}$	*RN*	$T_{mid\text{-}way}$	*RN*	$T_{mid\text{-}way}$	*RN*	$T_{mid\text{-}way}$
1	0.5322	12	1.3702	23	0.8067	34	1.8819	45	0.7579	56	1.1212
2	0.3319	13	1.0416	24	0.7487	35	1.3958	46	0.8175	57	0.9590
3	0.3456	14	1.5066	25	1.9047	36	1.4950	47	0.9958	58	1.1340
4	0.3059	15	0.9574	26	0.5739	37	0.8313	48	0.6634	59	0.6324
5	0.2905	16	0.7860	27	0.6635	38	0.9175	49	1.9213	60	0.6771
6	0.4372	17	0.7142	28	1.4150	39	1.3894	50	0.8105	61	0.4352
7	0.5472	18	0.5670	29	0.8789	40	1.3627	51	1.6760	62	0.6032
8	0.6316	19	0.9864	30	1.0308	41	1.1264	52	1.7268	63	1.2369
9	0.6250	20	0.9843	31	1.8297	42	0.9812	53	0.9794	64	0.7166
10	0.8273	21	0.7430	32	1.2414	43	0.7597	54	0.8929	65	0.4582
11	0.6099	22	1.0092	33	1.5729	44	0.8254	55	0.9548	66	0.3359
Sum:		62.2919 s									

responsible to protect the same feeder (L_1) and R_{52} is the backup protection for R_{57}. In this case, the coordination between R_{57}-R_{52} is obtained for the faults occur in front of R_{57} with a constant network topology using the conventional coordination scheme. However, this assumption is incorrect for the faults occurring far from R_{57} and close to R_{58}, because R_{58} is likely to react before R_{57} in such cases.

Therefore, a network reconfiguration is expected during the fault instant. In other words, for the case that the fault occurs close to the R_{57}, DOCR will react before R_{58} and the network configuration will remain similar to faulty instant and the conventional coordination methods are effective. However, for the case that fault occurs close to R_{58}, DOCR will react before R_{57} and the network reconfiguration will be possible during a faulty instant. Consequently, the applied coordination scheme should protect the power system for both cases. To evaluate the proposed method performance for this coordination issue, three possible scenarios can be taken into account for the faults between R_{57} and R_{58}.

The first possible scenario is that R_{57} trips before R_{58} once the fault is close to R_{57}, or R_{58} fails to trip. In this scenario, there is no reconfiguration in the power network and the proposed method can satisfy reliable protection. The second scenario is that R_{58} trips before R_{57} for a fault between R_{57} and R_{58}. In this scenario, a network reconfiguration is inevitable and all the seen currents by R_{57} (main protection) and R_{52} (backup protection) will change suddenly from the values tuned for coordination. Therefore, the behavior of R_{57} and R_{52} under these unexpected changes in the measured currents should be analyzed. It should be mentioned that the network reconfiguration often leads to increase the measured current by R_{57}. In other words, before the reaction of the R_{58}, the fault current is fed through both R_{57} and R_{58}, and after reaction of R_{58}, the fault is fed only through R_{57}. Consequently, the R_{57} becomes more sensitive and no extra protection issue is exposed to R_{57} considering the minimum operating time of 0.05 s. In addition, if the current seen by the backup protection (R_{52}) decreases, the pair R_{57}-R_{52} will change from case C to case D and consequently, the conventional protection scheme fails to satisfy desirable coordination for this case. Fortunately, reliable coordination between R_{57}-R_{52} is guaranteed for this condition via a communication link using the proposed method. It also worth noting that, if the current seen by the backup protection (R_{52}) increases, no extra side effect is imposed on the pair R_{57}-R_{52}.

5. Conclusion

In this research work, undesirable relay pairs which cannot be coordinated by non-communication scheme were identified, firstly. Afterwards, the communication links to preserve desirable coordination were proposed, and then a novel optimization method were applied to address overcurrent coordination problem and protect the power system against both near- and far-end faults. It was demonstrated that the proposed optimizer can effectively guarantee the transient stability of synchronous generators and the results can meet criteria and provide satisfaction. The performance and the strength of the proposed method were demonstrated and discussed through different simulation studies over both distribution and transmission networks. As a conclusion, appropriate characteristics with nonstandard curves can become superior and provide highly desirable performance rather than standard relays in many cases. Moreover, transient stability of synchronous generators is unfeasible after de-energizing the line in some cases. That is the reason, the synchronous generators can become unstable even for transient faults.

CRediT authorship contribution statement

A. Darabi: Conceptualization, Methodology, Software, Validation, Writing - original draft. **M. Bagheri:** Writing - review & editing, Supervision, Funding acquisition. **G.B. Gharehpetian:** Writing - review & editing, Supervision.

Declaration of Competing Interest

The authors declare that they have no known competing financial interests or personal relationships that could have appeared to influence the work reported in this paper.

Acknowledgments

This work was supported in part by the Program-Targeted Funding of the Ministry of Education and Science of the Republic of Kazakhstan through the Innovative Materials and Systems for Energy Conversion and Storage for 2018–2020 under Grant BR05236524.

References

[1] Nabab Alam M. Adaptive protection coordination scheme using numerical directional overcurrent relays. IEEE Trans Ind Informat 2019;15(1):64–73.
[2] Liu L, Fu L. Minimum break point set determination for directional overcurrent relay coordination in large scale power networks via matrix computations. IEEE Trans Power Del 2017;32(4):1784–9.
[3] Wan Hui. An adaptive multiagent approach to protection relay coordination with distributed generators in industrial power distribution system. IEEE Trans Ind Appl 2010;46(5):2118–24.
[4] Yazdanpanahi H, et al. A new control strategy to mitigate the impact of inverter-based DGs on protection system. IEEE Trans Smart Grid 2012;3(3):1427–36.
[5] Zeineldin HH. Optimal protection coordination for meshed distribution systems with DG using dual setting directional over-current relays. IEEE Trans Smart Grid 2015;6(1):115–23.
[6] Solati Alkaran D. Optimal overcurrent relay coordination in interconnected networks by using fuzzy-based GA method. IEEE Trans Smart Grid 2018;9(4):3091–101.
[7] Sharaf HM, et al. Protection coordination for microgrids with grid-connected and islanded capabilities using communication assisted dual setting directional overcurrent relays. IEEE Trans Smart Grid 2018;9(1):143–51.
[8] Nikolaidis VC, Papanikolaou E, Safigianni AS. A communication-assisted overcurrent protection scheme for radial distribution systems with distributed generation. IEEE Trans Smart Grid 2016;7(1):114–23. https://doi.org/10.1109/TSG.2015.2411216.
[9] Abdi-Khorsand M, Vittal V. Modeling protection systems in time-domain simulations: a new method to detect mis-operating relays for unstable power swings. IEEE Trans Power Syst 2017;32(4):2790–8.
[10] Yen Shih M. An adaptive overcurrent coordination scheme to improve relay sensitivity and overcome drawbacks due to distributed generation in smart grids. IEEE Trans Ind Appl 2017.;53(6):5217–28.
[11] Meneses CAP, Mantovani JRS. Improving the grid operation and reliability cost of distribution systems with dispersed generation. IEEE Trans Power Syst 2013;28(3):2485–96.
[12] Ojaghi M, Mohammadi V. Use of clustering to reduce the number of different setting groups for adaptive coordination of overcurrent relays. IEEE Trans. Power Del. 2018;33(3):1204–12.
[13] Huchel Ł, Zeineldin HH. Planning the coordination of directional overcurrent relays for distribution systems considering DG. IEEE Trans Smart Grid 2016;7(3):1642–9.
[14] Purwar Ekta, Vishwakarma DN, Singh SP. A novel constraints reduction-based optimal relay coordination method considering variable operational status of distribution system with DGs. IEEE Trans Smart Grid 2019;10(1):889–98. https://doi.org/10.1109/TSG.2017.2754399.
[15] Momesso Antonio EC, Bernardes WMS, Asada Eduardo N. Fuzzy adaptive setting for time-current-voltage based overcurrent relays in distribution systems. Int J Electr Power Energy Syst 2019;108:135–44.
[16] Chen Li-Hsiung. Overcurrent protection for distribution feeders with renewable generation. Int J Electr Power Energy Syst 2017;84:202–13.
[17] Seyedi Y, Karimi H. Coordinated protection and control based on synchro-phasor data processing in smart distribution networks. IEEE Trans Power Syst 2018;33(1):634–45.
[18] Pandi VR, et al. Determining optimal location and size of distributed generation resources considering harmonic and protection coordination limits. IEEE Trans Power Syst 2013;28(2). 1245-1254.
[19] Khanbabapour S, Hamedani Golshan MS. Synchronous DG planning for simultaneous improvement of technical, overcurrent and timely anti-islanding protection indices of the network to preserve protection coordination. IEEE Trans Power Del 2017;32(1):474–83.
[20] Ghanbari T, Farjah E. Unidirectional fault current limiter: an efficient interface between the microgrid and main network. IEEE Trans Power Syst 2013;28(2):1591–8.
[21] Yang H. Placement of fault current limiters in a power system through a two-stage optimization approach. IEEE Trans Power Syst 2018;33(1):131–40.
[22] Fattaheian-Dehkordi S, et al. Transmission system critical component identification considering full substations configuration and protection systems. IEEE Trans Power Syst 2018;33(5):5365–73.
[23] Meyer R, Zlotnik A, Mertens A. Fault ride through control of medium-voltage converters with LCL filter in distributed generation systems. IEEE Trans Ind Appl

2014;50(5):3448–56.
[24] Salem MM. Modified inverter control of distributed generation for enhanced relaying coordination in distribution networks. IEEE Trans Power Del 2017;32(1):78–87.
[25] Piya P. Fault ride-through capability of voltage-controlled inverters. IEEE Trans Ind Electron 2018;65(10):7933–43.
[26] Hamidi ME, Mohammadi Chabanloo R. Optimal allocation of distributed generation with optimal sizing of fault current limiter to reduce the impact on distribution networks using NSGA-II. IEEE Syst J 2019;13(2):1714–24.
[27] Rebizant W, Solak K, Brusilowicz B, Benysek G, Kempski A, Rusinski J. Coordination of overcurrent protection relays in networks with superconducting fault current limiters. Int J Electr Power Energy Syst 2018;95:307–14.
[28] Mohammadi Chabanlooa R, Ghotbi Malekia M, Mohammad Mousavi Agahb S, Mokhtarpour Habashic E. Comprehensive coordination of radial distribution network protection in the presence of synchronous distributed generation using fault current limiter. Int J Electr Power Energy Syst 2018;99:214–24.
[29] Conti Stefania. Analysis of distribution network protection issues in presence of dispersed generation. Electr Power Syst Res 2009;79:49–56.
[30] Pereira K. A multi-objective optimization technique to develop protection systems of distribution networks with distributed generation. IEEE Trans Power Syst 2018;33(6):7064–75.
[31] Soleymani Aghdam T. Transient stability constrained protection coordination for distribution systems with DG. IEEE Trans Smart Grid 2018;9(6):5733–41.
[32] Amraee T. Coordination of directional overcurrent relays using seeker algorithm. IEEE Trans Power Del 2012;27(3):1415–22.
[33] Srivastava A. Optimal coordination of overcurrent relays using gravitational search algorithm with DG penetration. IEEE Trans Ind Appl 2018;54(2):1155–65.
[34] Mansour MM. A modified particle swarm optimizer for the coordination of directional overcurrent relays. IEEE Trans Power Del 2007;22(3):1400–10.
[35] Mohammadi R. Overcurrent relays coordination considering the priority of constraints. IEEE Trans Power Del 2011;26(3):1927–38.
[36] Bedekar PP, Bhide SR. Optimum coordination of directional overcurrent relays using the hybrid GA-NLP approach. IEEE Trans Power Del 2011;26(1):109–19.
[37] Saberi Noghabi A. Considering different network topologies in optimal overcurrent relay coordination using a hybrid GA. IEEE Trans Power Del 2009;24(4):1857–63.
[38] Darabi A, et al. Highly accurate directional overcurrent coordination via combination of Rosen's gradient projection- complex method with GA-PSO algorithm. IEEE Syst J 2019:1–12.
[39] Jamali S, Borhani-Bahabadi H. Non-communication protection method for meshed and radial distribution networks with synchronous-based DG. Int J Electr Power Energy Syst 2017;93:468–78.
[40] Ahmadi SA, Karami H, Gharehpetian GB. Comprehensive coordination of combined directional overcurrent and distance relays considering miscoordination reduction. Int J Electr Power Energy Syst 2017;92:42–52.
[41] Ahmadi SA, Karami H, Sanjari MJ, Tarimoradi H, Gharehpetian GB. Application of hyper-spherical search algorithm for optimal coordination of overcurrent relays considering different relay characteristics. Int J Electr Power Energy Syst 2016;83:443–9.
[42] Chelliah TR, Thangaraj R, Allamsetty S, Millie Pant. Coordination of directional overcurrent relays using opposition based chaotic differential evolution algorithm. Int J Electr Power Energy Syst 2014;55:341–50.
[43] Gokhale SS, Kale VS. An application of a tent map initiated Chaotic Firefly algorithm for optimal overcurrent relay coordination. Int J Electr Power Energy Syst 2016;78:336–42.
[44] Thakur M, Kumar A. Optimal coordination of directional over current relays using a modified real coded genetic algorithm: a comparative study. Int J Electr Power Energy Syst 2016;82:484–95.
[45] Chen ChR, Hung Lee Ch, Chi J, Chang. Optimal overcurrent relay coordination in power distribution system using a new approach. Int J Electr Power Energy Syst 2013;45:217–22.
[46] Singh M, Panigrahi BK, Abhyankar AR. Optimal coordination of directional overcurrent relays using Teaching Learning-Based Optimization (TLBO) algorithm. Int J Electr Power Energy Syst 2013;50:33–41.
[47] Mohamed Sharaf H, Zeineldin HH, Ibrahim DKh, EL-Din E, Abou EL-Zahab. A proposed coordination strategy for meshed distribution systems with DG considering user-defined characteristics of directional inverse time overcurrent relays. Int J Electr Power Energy Syst 2015;65:49–58.
[48] Nabab Alam M, Das B, Pant V. An interior point method based protection coordination scheme for directional overcurrent relays in meshed networks. Int J Electr Power Energy Syst 2016;81:153–64.
[49] Sueiro José A, Diaz-Dorado E, Míguez E, José Cidrás. Coordination of directional overcurrent relay using evolutionary algorithm and linear programming. Int J Electr Power Energy Syst 2012;42:299–305.
[50] Rajput Vipul N, Pandya Kartik S. Coordination of directional overcurrent relays in the interconnected power systems using effective tuning of harmony search algorithm. Sustain Comput Inf Syst 2017;15:1–15.
[51] Rajput Vipul N, Adelnia Farhad, Pandya Kartik S. Optimal coordination of directional overcurrent relays using improved mathematical formulation. In: IET generation, transmission & distribution, vol. 12, no. 9; 15 5 2018. p. 2086–94.
[52] Armentano R, et al. The internet of things: foundation for smart cities, EHealth, and ubiquitous computing. 1st ed. CRC Press; 2017.
[53] Samet H, et al. Efficient current-based directional relay algorithm. IEEE Syst J 2019;13(2):1262–72.
[54] Rao SS. Engineering optimization: theory and practice, 4th ed.; Jul. 2009.
[55] Darabi A, et al. Dual feasible direction- finding nonlinear programming combined with metaheuristic approaches for exact overcurrent relay coordination. Int J Electr Power Energy Syst 2020;114.
[56] Saleh KA, Zeineldin HH, Al-Hinai A, El-Saadany EF. Optimal coordination of directional overcurrent relays using a new time–current–voltage characteristic. IEEE Trans Power Del 2015;30(2):537–44. https://doi.org/10.1109/TPWRD.2014.2341666.
[57] Gers J, Holmes E. Protection of electricity distribution networks. ser. IET power and energy series. 3rd ed. Institution of Engineering and Technology; 2011.
[58] Available [online]: https://www2.ee.washington.edu/research/pstca/.
[59] Papaspiliotopoulos VA, et al. A novel quadratically constrained quadratic programming method for optimal coordination of directional overcurrent relays. IEEE Trans. Power Del. 2017;32(1):3–10.
[60] Grainger JJ, Stevenson WD. Power system analysis; Jan. 1994.
[61] Naiem AF, Hegazy Y, Abdelaziz AY, Elsharkawy MA. A classification technique for recloser-fuse coordination in distribution systems with distributed generation. IEEE Trans Power Del 2012;27(1):176–85. https://doi.org/10.1109/TPWRD.2011.2170224.
[62] Santoso S, Short TA. Identification of fuse and recloser operations in a radial distribution system. IEEE Trans Power Del 2007;22(4):2370–7.
[63] Wheeler KA. A novel reclosing scheme for mitigation of distributed generation effects on overcurrent protection. IEEE Trans Power Del 2018;33(2):981–91.